



Studying sprouting angiogenesis under combination of oxygen gradients and co-culture of fibroblasts using microfluidic cell culture model



Heng-Hua Hsu^{a,b}, Ping-Liang Ko^{a,c}, Chien-Chung Peng^a, Ya-Jen Cheng^{d,e}, Hsiao-Mei Wu^f, Yi-Chung Tung^{a,g,*}

^a Research Center of Applied Sciences, Academia Sinica, Taipei, Taiwan

^b Department of Engineering and System Science, National Tsing Hua University, Hsinchu, Taiwan

^c Department of Mechanical Engineering, National Taiwan University, Taipei, Taiwan

^d Institute of Molecular Biology, Academia Sinica, Taipei, Taiwan

^e Neuroscience Program of Academia Sinica, Academia Sinica, Taipei, Taiwan

^f Department of Biomechanics Engineering, National Taiwan University, Taipei, Taiwan

^g College of Engineering, Chang Gung University, Taoyuan, Taiwan

ARTICLE INFO

Keywords:

Sprouting angiogenesis
Oxygen gradients
Cell co-culture
Fibroblast
Microfluidics

ABSTRACT

Sprouting angiogenesis is an essential process for expanding vascular systems under various physiological and pathological conditions. In this paper, a microfluidic device capable of integrating a hydrogel matrix for cell culture and generating stable oxygen gradients is developed to study the sprouting angiogenesis of endothelial cells under combinations of oxygen gradients and co-culture of fibroblast cells. The endothelial cells can be cultured as a monolayer endothelium inside the device to mimic an existing blood vessel, and the hydrogel without or with fibroblast cells cultured in it provides a matrix next to the formed endothelium for three-dimensional sprouting of the endothelial cells. Oxygen gradients can be stably established inside the device for cell culture using the spatially-confined chemical reaction method. Using the device, the sprouting angiogenesis under combinations of oxygen gradients and co-culture of fibroblast cells is systematically studied. The results show that the oxygen gradient and the co-culture of fibroblast cells in the hydrogel can promote sprouting of the endothelial cells into the hydrogel matrix by altering cytokines in the culture medium and the physical properties of the hydrogel. The developed device provides a powerful *in vitro* model to investigate sprouting angiogenesis under various *in vivo*-like microenvironments.

1. Introduction

Sprouting angiogenesis is the growth of new blood vessels from pre-existing ones [1], and the angiogenic vessel network formation is essential for expanding the vascular systems. The scale of the vascular network expands is according to the response of demanding changes in metabolism during physiological organ growth in order to supply sufficient oxygen and nutrients [2]. Sprouting angiogenesis occurs continuously in both physiological and pathological developments throughout the lifespan. During the process, angiogenesis can be affected by many biological, chemical, and physical factors. For instance, vascular endothelial growth factor (VEGF) has been identified as a primary key regulator to dynamically adjust the angiogenic sprouting behaviors [3]. Also, change of metabolic signaling in cells can activate the different cellular

responses during the angiogenic formations [4,5]. In addition, the physical properties of the matrix around the blood vessels also play important roles in regulating angiogenesis, and it has been found that the increase in matrix stiffness can promote angiogenesis [6].

Among various factors, oxygen is one of the essential factors capable of regulating sprouting angiogenesis from different perspectives. Oxygen has been identified as a crucial factor for cellular metabolism and bioenergetic processes, and oxygen further regulates various sprouting angiogenesis behaviors [7–9]. In recent decades, the hypoxic cellular microenvironment has been identified as a driving factor of sprouting angiogenesis through the hypoxia induced factor (HIF) pathway. Prolonged stabilization of HIF during hypoxia promotes various pro-angiogenic pathways involving interactions between endothelial and stromal cells during both physiological and pathological vascular

* Corresponding author. Research Center of Applied Sciences, Academia Sinica, Taipei, Taiwan.

E-mail address: tungy@gate.sinica.edu.tw (Y.-C. Tung).

<https://doi.org/10.1016/j.mtbio.2023.100703>

Received 13 March 2023; Received in revised form 24 May 2023; Accepted 12 June 2023

Available online 1 July 2023

2590-0064/© 2023 The Authors. Published by Elsevier Ltd. This is an open access article under the CC BY-NC-ND license (<http://creativecommons.org/licenses/by-nc-nd/4.0/>).

development [10,11]. In addition, stromal cells in the neighboring areas around the blood vessels and their secreted cytokines also play essential roles in regulating sprouting angiogenesis and the vessel lumen formation *in vivo*. The cytokines secreted from fibroblasts such as angiopoietin-1, angiogenin, and hepatocyte growth factor (HGF), have been found to promote endothelial cell sprouting [12]. Also, the presence of fibroblast cells in the matrix results in significantly stiffer matrix that has been found to enhance the lumen formation [12]. In addition, hypoxia has also been found to induce extracellular matrix (ECM) remodeling and further alter the matrix stiffness that promotes angiogenic migration and sprouting of endothelial and stromal cells [13,14]. As a result, the oxygen microenvironment, stromal cells, and their interaction can greatly affect the sprouting angiogenesis during the new blood vessel formation through various mechanisms.

However, oxygen tension is usually not uniform *in vivo* due to the arrangement of heterogeneous cell types and various biological activities, and the direct effects of oxygen gradients on the sprouting angiogenesis are seldom studied due to lack of reliable cell culture platforms capable of consistently generating oxygen gradients without tedious operation and complex instrumentation. Recently, a variety of three-dimensional *in vitro* cell culture models have been developed due to their capability of reconstituting similar *in vivo* microenvironments. The models can provide more insightful information comparing to conventional monolayer cell culture models [15].

Among various models, microfluidic cell culture devices have been broadly exploited to construct *in vitro* models due to their great controllability of cell culture microenvironments and the possibility for automation and scale-up [16–19]. Recently, several microfluidic devices have also been developed to control oxygen tensions and generate oxygen gradients for cell culture in two- and three-dimensional manners [20]. However, most of the devices rely on direct chemical addition or gas purging for oxygen gradient generation which may alter the cellular responses or introduce undesired bubbles for cell culture, respectively. In this paper, a microfluidic device capable of consistently generating oxygen gradients is developed. The oxygen gradient is generated using the previously developed spatially-confined chemical reaction method with a simple setup, short transient time, long-term stability, and cell culture incubator compatibility [21–24]. The device also allows a three-dimensional hydrogel matrix to be embedded into a microfluidic channel for cell culture and sprouting angiogenesis study [25,26]. The established oxygen gradients are quantitatively characterized using an oxygen sensitive fluorescence dye with fluorescence lifetime-based measurement, and the sprouting angiogenesis of endothelial cells is characterized based on image analysis. Exploiting the device, the direct effects of oxygen gradients, neighboring stromal cells, and matrix remodeling on sprouting angiogenesis can be better studied *in vitro*.

In the experiments, endothelial cells are cultured as a mono-layer to mimic an existing endothelium in a blood vessel, and a hydrogel matrix is placed next to the endothelium for three-dimensional sprouting angiogenesis. The effects of oxygen gradients on sprouting angiogenesis are first studied using the devices with different dimensions to generate various oxygen gradients. In order to further investigate the effects of the stromal cells, fibroblast cells are cultured in the hydrogel matrix for the study. The angiogenesis sprouting of the endothelium is quantified by analyzing the captured microscopic images, and angiogenesis cytokine array analysis is also performed to explore the possible underlying mechanisms. Moreover, the physical properties of the hydrogel are characterized using atomic force microscopy (AFM) to observe the matrix remodeling. The experimental results demonstrate the functions of the designed device, and confirm the critical roles of oxygen gradients and fibroblast cells on cytokine secretion and matrix remodeling that can greatly affect sprouting angiogenesis. The developed device provides a simple yet powerful platform to study sprouting angiogenesis and more interesting biological activities under controlled oxygen gradients. Furthermore, the experimental results provide insightful information and may open a new window for sprouting angiogenesis research.

2. Materials and methods

2.1. Device design and fabrication

In order to perform cell culture under controlled oxygen gradients, a microfluidic device is designed and fabricated in the experiments. The microfluidic device (Fig. 1) consists of two layers of polydimethylsiloxane (PDMS) (Sylgard 184, Dow Corning, Midland, MI). The top layer is designed with patterns of three microfluidic channel sets including a cell culture channel, a hydrogel channel, and an oxygen scavenging channel as shown in Fig. 1(a). The bottom layer is a PDMS-coated glass slide to be sealed against the top layer forming the microfluidic channels. In the experiments, the endothelial cells are cultured in the cell culture channel (width: 800 μm , height: 100 μm) as a mono-layer, and the hydrogel is introduced into the hydrogel channel (width: 200 μm , height: 100 μm) as a three-dimensional matrix into which the endothelial cells sprout for angiogenic vessel formation. The cell culture channel and the hydrogel channel are separated by a line of trapezoid pillars to confine the hydrogel in the hydrogel channel while allowing direct contact to the endothelial cells on the interface. The oxygen scavenging channel is designed with two inlets and one outlet to generate the oxygen gradient in the neighboring channels using the previously developed spatially-confined chemical reaction method [22–24]. The hydrogel channel and the oxygen scavenging channel are separated by a PDMS thin wall with three different widths (50 μm , 75 μm , and 100 μm) to generate different oxygen gradients inside the cell culture and hydrogel channels.

The top layer is fabricated utilizing the well-developed soft lithography replica molding technique [22]. The master mold with negative relief features is fabricated by patterning a negative tone photoresist (SU-8 2050, MicroChem, Newton, MA) on a silicon wafer using conventional photolithography. The mold is then silanized using 1H,1H,2H,2H-perfluorooctyl trichlorosilane (97%) (L16606, Alfa Aesar, Ward Hill, MA) in a desiccator to prevent undesired bonding between the mold and PDMS [27]. The PDMS prepolymer made of a mixture of base and curing agent with a 10:1 (w/w) ratio is then poured onto the mold and cured in a 65 °C oven for more than 4 h. After curing, all the inlets and outlets are punched using a biopsy punch with a diameter of 1.5 mm. The bottom layer is prepared by spinning the PDMS prepolymer onto a glass slide to form a 30 μm -thick layer of PDMS. To assemble the entire device, the top PDMS layer and the bottom PDMS-coated glass slide are aligned and irreversibly bonded using an oxygen plasma surface treatment (90 W) for 30 s (PX-250, Nordson MARCH, Concord, CA) (Fig. 1(b)). The fabricated devices are sterilized by UV exposure for 30 min before performing the cell experiments.

2.2. Cell culture

To investigate sprouting angiogenesis of endothelial cells into the three-dimensional hydrogel matrix, human umbilical vein endothelial cells (HUVECs) (EndoGRO™ Normal HUVEC, SCCE001, Millipore, USA) are utilized. HUVECs have been broadly exploited to construct *in vitro* models to investigate endothelial angiogenic sprouting and tubular capillary network formation [28,29]. In the experiments, the HUVEC cells are cultured using a commercially available growth medium (EndoGRO™ Media Products for Human Endothelial Cell Culture, SCME002, Millipore, USA). To further study the effects of stromal cells on the sprouting angiogenesis of the endothelial cells, a human fetal lung fibroblast cell line (MRC-5) cultured using a growth medium (MEM medium, Gibco 41,090, Invitrogen Co., Carlsbad, CA) with 10% v/v fetal bovine serum (FBS) (Gibco 10,082, Invitrogen Co.) and 1% v/v antibiotic-antimycotic (Gibco 15,240, Invitrogen Co.) is exploited in the experiments. MRC-5 cells have also been broadly used for *in vitro* cell co-culture models due to their well-studied properties. Moreover, co-culture of HUVEC and MRC-5 has also been used to investigate interactions between endothelial cells and fibroblasts [30]. The stocks of

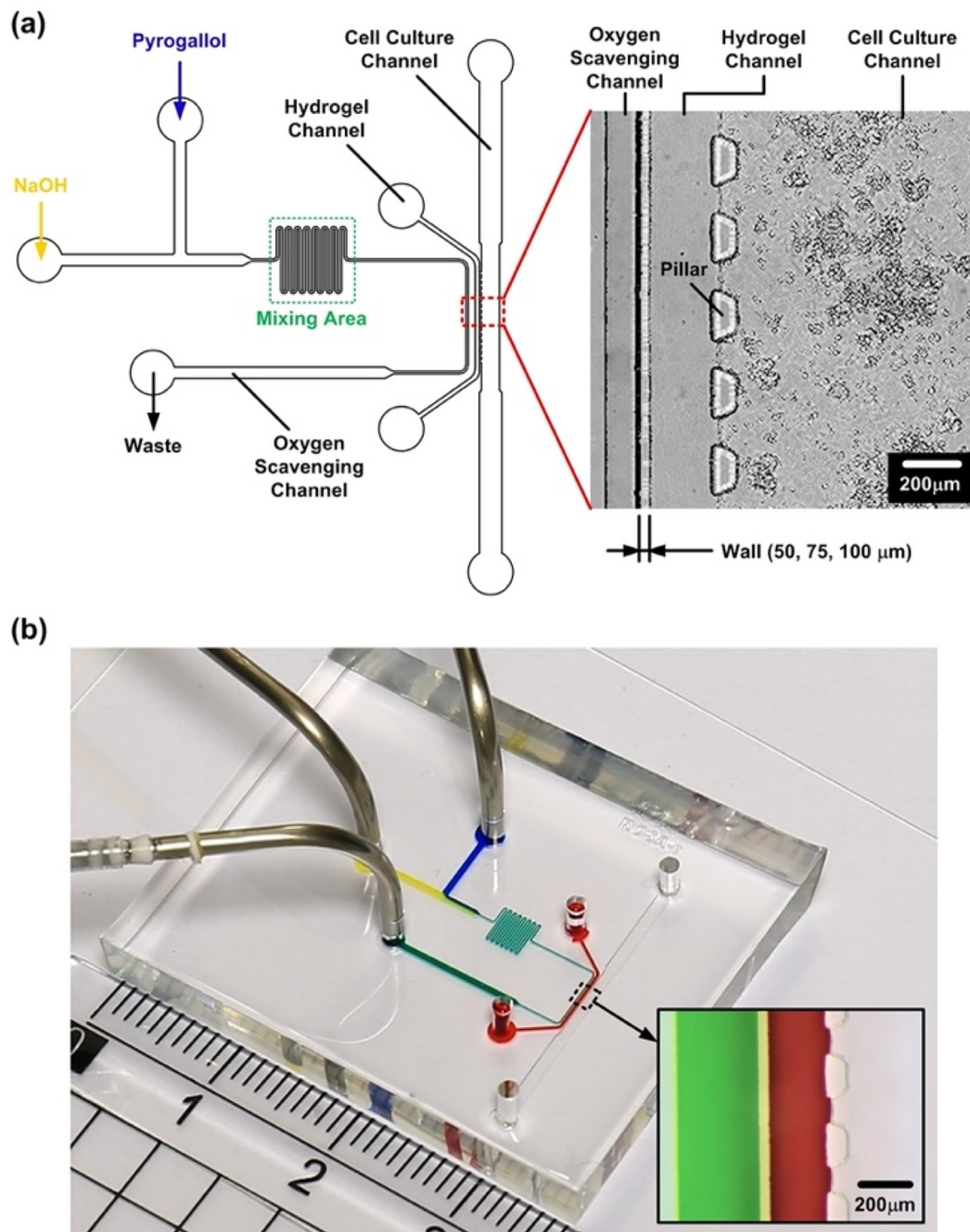


Fig. 1. (a) The schematic of the designed microfluidic device to perform the experiments investigating endothelial cell sprouting into hydrogels under various controlled oxygen microenvironment and cell co-culture conditions. The oxygen gradients are generated using the devices with different wall widths (50 μm , 75 μm and 100 μm) between the oxygen scavenging channel and the hydrogel channel. (b) Photo of the fabricated microfluidic device (wall width: 50 μm) filled with food dyes.

both cells are maintained in T75 cell culture flasks at 37°C in a humidified incubator with 5% CO₂. The growth media are changed one day after the passage, and the cells are sub-cultured every three days. The cells are passaged by dissociating the cells with 0.25% TrypLE Express (Gibco 12,605, Thermo Fisher Scientific, USA). The cell suspensions for the experiments are prepared by centrifuging the dissociated cells at 1000 rpm for 5 min at room temperature and resuspending the cells with desired densities using the according growth media. For consistent experimental results, the HUVECs and MRC-5 cells with passages 3 to 5 and 28 to 33 are used in all the experiments, respectively.

2.3. Three-dimensional hydrogel matrix formation

In order to construct an *in vivo*-like three-dimensional matrix for sprouting angiogenesis of the endothelial cells, fibrinogen from human plasma (F3879, Sigma-Aldrich, St. Louis, MO, USA) is exploited as the hydrogel matrix in the experiments. The hydrogel solution contains 100 μl human fibrinogen solution with a concentration of 1 mg per 75 μl of EndoGRO™ Media (SCME002, Millipore, USA), 2.5 μl Aprotinin with a concentration of 30 U/ml (A3428, Sigma-Aldrich, St. Louis, MO, USA), and 25 μl Thrombin with a concentration of 25U/ml (T6884, Sigma-Aldrich, St. Louis, MO, USA). To further investigate the effects of the

stromal cells on the sprouting angiogenesis, the lung fibroblast (MRC-5) cells are mixed into the hydrogel solution with a density of 10^6 cells/ml for the experiments. After preparing the hydrogel solution, 100 μ l of the solution without or with the MRC-5 cells is then introduced into the hydrogel channel and incubated for 10 min at 37 °C to cure the hydrogel. After curing the hydrogel, 200 μ l of the cell growth medium is injected into the channels to prevent drying of the hydrogel.

2.4. Oxygen gradients generation and characterization

In order to investigate the endothelial sprouting under different oxygen microenvironments, the oxygen gradient is generated in the microfluidic device using the spatially-confined method [22]. In the experiments, pyrogallol (benzene-1,2,3-triol, $C_6H_6O_3$) (87-66-1, Alfa Aesar, Ward Hill, MA) and sodium hydroxide (NaOH) (30,620, Sigma-Aldrich, St Louis, MO) solutions are introduced into the oxygen scavenging channel from the two separate inlets. The two solutions are mixed when flowing into the serpentine channel, and pyrogallol can rapidly absorb oxygen when in an alkaline solution. In the experiments, the pyrogallol (50 mg/ml) and NaOH (1 M) solutions are introduced into the channel with flow rates of 0.5 μ l/min for the oxygen scavenging chemical reaction. It is noticed that only 0.72 ml of each chemical is required for a 24-h experimental period, which can greatly reduce chemical consumption and the oxygen scavenging method is suitable for long-term cell experiments.

To characterize the oxygen gradients generated inside the hydrogel and cell culture channels, an oxygen sensitive fluorescence dye, tris (2,2'-bipyridyl) ruthenium (II) chloride hexahydrate (5 mg/ml) (50525-27-4, Acros Organics, Geel, Belgium), is utilized as an oxygen sensor in the experiments. The ruthenium-based fluorescent dye provides great photostability and is specifically sensitive to oxygen variation without known complex in the ground state with different lifetime [23,31,32]. Since the fluorescence lifetime of the dye can be shortened by the presence of oxygen, the oxygen gradient profiles are estimated using the lifetime measurement. The lifetime measurement provides a more precise and reliable quantitative method due to its insensitivity to ambient optical noise. According to the Stern–Volmer equation, the quantitative oxygen concentration can be calculated as

$$[O_2] = \frac{1}{K_q} \left(\frac{\tau_0}{\tau} - 1 \right)$$

where τ_0 and τ are the fluorescence lifetimes without and with the presence of oxygen, respectively, and K_q is the quenching constant. For quantification of oxygen tension values, a fluorescence image of a droplet of the dye in an ambient environment with oxygen tension of approximately 20.9% is used as a reference with the fluorescence lifetime of 381 ns in the experiments [32].

For the oxygen tension measurement inside the microfluidic device, the microfluidic device is treated with oxygen plasma to make the channel surfaces hydrophilic. The hydrogel matrix is first formed in the hydrogel channel of the device. In addition, the pure H_2O is introduced to fill up the cell culture channel for maintaining the hydrophilic condition before injection of the oxygen sensitive dye. Afterwards, the oxygen sensitive dye solution is then introduced (flow rate: 5 μ l/min) into the cell culture channel by a syringe pump for 10 min to allow the dye diffusion into the hydrogel and kept static for more than 2 min for the measurement. The pyrogallol and NaOH solution are then introduced into the oxygen scavenging channel using a syringe pump for the measurement. The measurements are performed under the normoxic (21% O_2) condition, and the detailed measurement setup is described in the Supplementary Information (Fig. S1).

2.5. Sprouting angiogenesis assay

To perform the sprouting angiogenesis assay, the cell culture channel

is first treated with 50 μ l of ECM protein, fibronectin (FC010, Merck KGaA, Darmstadt, Germany), with a concentration of 0.1 mg/ml for 2 h at 37 °C to promote the cell adhesion after the hydrogel matrix formation. The fibronectin solution is replaced by the complete growth medium after the treatment, and the HUVECs (30 μ l with a cell density of 10^7 cells/ml) are then seeded into the cell culture channel. The HUVECs are cultured for more than 3 h in the devices before applying the oxygen gradients, and the entire cell experiments are performed for more than 72 h.

2.6. Angiogenic sprouting length analysis

To quantitatively estimate the length of which the HUVECs sprout into the hydrogel under different oxygen gradients and co-culture conditions, image analysis is performed on the brightfield images captured using an inverted fluorescence microscope (DMi8, Leica Microsystems, Wetzlar, Germany). The image analysis is achieved using a computer code programmed on a commercially available mathematics software, Matlab (R2019b, The Math Works, Inc., Natick, MA). The length of sprouting angiogenesis (L_{SA}) is defined as $L_{SA} = A/L$, where A and L are sprouting angiogenesis area and channel length, respectively (Fig. 2). The estimated sprouting angiogenesis length is helpful for investigating the effects of oxygen gradients and co-culture conditions on the sprouting angiogenesis of the endothelial cells.

2.7. Cell viability assay

To confirm the cell compatibility of the device and confirm the viability of the HUVECs during their sprouting in the hydrogel under different culture conditions, the cells cultured in the devices for 72 h were stained using a fluorescence-based live/dead cytotoxicity assay (LIVE/DEAD Viability/Cytotoxicity kit, L3224, Thermo Fisher Scientific, USA). The live/dead stain solution contained Calcein AM (2 μ M), ethidium homodimer-1 (EthD-1) (2 μ M), and Hoechst 33,342 (50 μ l/ml) (NucBlue™ Live ReadyProbes™ Reagent, R37605, Invitrogen, USA) were introduced into the device and incubated for 45 min at 37 °C protected from light for the staining. The cell viability of the HUVECs is observed using an inverted fluorescence microscope (DMi8, Leica Microsystems, Wetzlar, Germany).

2.8. Immunocytochemistry staining

To observe the cytoskeleton and arrangement of HUVECs during the sprouting process, F-actin and adherens junction (VE-Cadherin) fluorescence staining is performed in the experiments. The cells are first fixed with 4% Paraformaldehyde (PFA, #15710 Electron Microscopy Sciences, Fisher Scientific, USA) for 30 min at room temperature and washed 3 times with DPBS. To permeabilize the cell membrane, the samples are treated with 0.1% Triton for 5 min at room temperature, and then washed 3 times with DPBS. Afterwards, the samples are treated with a blocking solution of 3% bovine serum albumin (BSA, A7906, Sigma-Aldrich Co.) in DPBS at 4°C overnight. The blocking solution is removed and the samples are incubated with the solution of VE-cadherin primary antibody at 4°C for overnight (1:250 with BSA solution, SC-9989, Santa Cruz Biotechnology Inc., Santa Cruz, CA). After 12–16 h, the paired secondary antibody Alexa Fluor 488 goat anti-mouse IgG antibody (1:800 with PBS, A-11,001, Thermo Fisher Scientific Inc.) is introduced for 1.5 h at room temperature. The solution is then aspirated and the samples are washed 3 times with DPBS. In addition, the staining solutions of F-actin in PBS (50 μ l/ml) (ActinRed™ 555 ReadyProbes® Reagent, R37112, Invitrogen, USA) and DAPI (50 μ l/ml) (NucBlue™ Fixed Cell ReadyProbes™ Reagent, R37606, Invitrogen, USA) are added into the samples in the dark for 1.5 h at room temperature.

Moreover, to investigate the influences of hydrogel-MRC-5 mixture solution on HUVECs during sprouting processes, MRC-5 has stained with cell tracker (1:1000 with cell culture medium; C34552, CellTracker Red

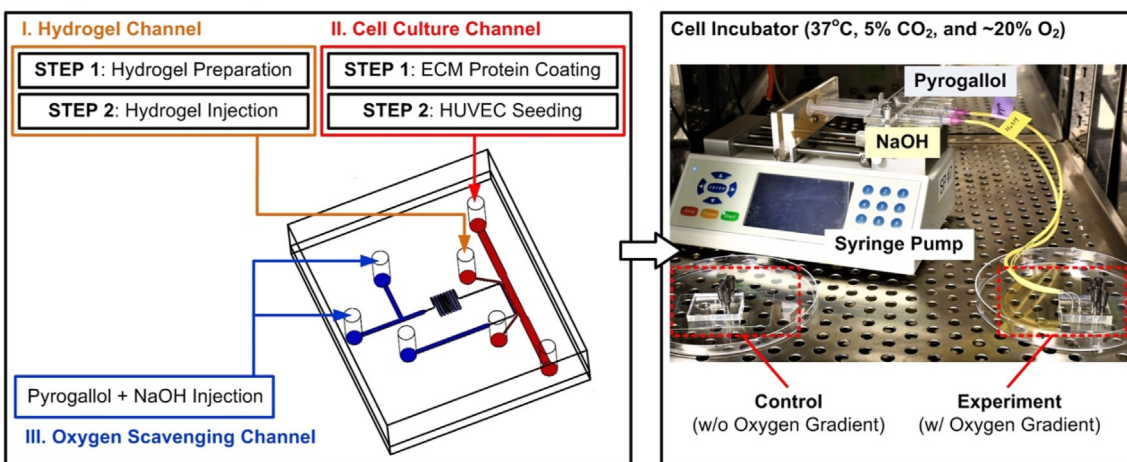
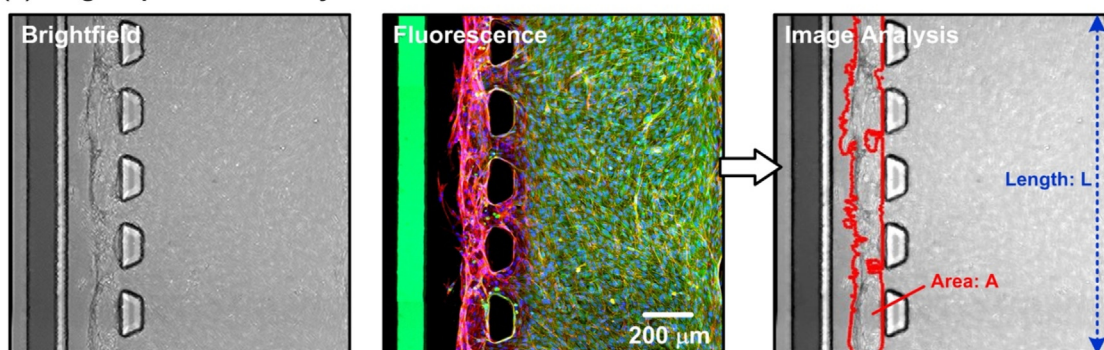
(a) Experimental Setup**(b) Image Acquisition and Analysis**

Fig. 2. (a) Experimental setup and photo for the cell sprouting experiments under normoxia and oxygen gradient microenvironments. The entire setup is placed in a humidified cell incubator supplied with 5% CO₂ and maintained at 37 °C. The oxygen gradient is generated inside the microfluidic device using the spatially confined chemical reaction method. Three different oxygen gradients are generated in the devices designed with the wall widths of 50 μm, 75 μm and 100 μm between the oxygen scavenging channel and the hydrogel channel. (b) The image acquisition and analysis method to estimate the average length of the cells sprouting into the hydrogel. Both brightfield and fluorescence images are acquired in the experiments, and the area of the cells sprouting into the hydrogel is automatically identified using a computer program for the average sprouting length estimation.

CMPX Dye, Invitrogen, USA) for 30 min before mixing with hydrogel then injected into the hydrogel channel of devices. After 72 h experimental period, samples are fixed, permeabilized, and blocked by using the same method as mentioned previously. Afterwards, in order to clarify the MRC-5 and HUVECs, samples are incubated with the solution of CD-31 primary antibody at 4 °C for overnight (ab76533, Abcam, dilution 1:250 with BSA). Next, the paired secondary antibody (1:800 with PBS; Invitrogen) is introduced for 1.5 h at room temperature, and the same DPBS wash protocol is processed. In addition, the staining solutions DAPI (50 μl/ml) (NucBlue™ Fixed Cell ReadyProbes™ Reagent, R37606, Invitrogen, USA) are added into the samples in the dark for 1.5 h at room temperature. The samples are washed 3 times with DPBS and visualized under a confocal laser scanning microscope (LSM 880, Carl Zeiss Microscopy GmbH, Oberkochen, Germany).

2.9. Cytokine array analysis

To investigate the possible molecular mechanisms of the effects from the co-culture and oxygen microenvironments, cytokine assay analysis is performed on the medium collected from the microfluidic device on Day 3. The conditioned medium is collected from HUVEC without or with MRC-5 co-culture for analysis using the human angiogenesis antibody array (Human Angiogenesis Antibody Array C1000, RayBiotech, Inc., Peachtree Corners, GA). The detailed information and results of the cytokine array exploited in the experiments are described in Fig. S2(a) in the Supplementary Information. The analysis is performed according to

the instructions provided by the manufacturer. Briefly, 2 ml of the blocking buffer is pipetted into the well with the angiogenesis antibody array membrane and incubated for 30 min at room temperature. After the incubation, the blocking buffer is removed, and the antibody membrane is washed twice with the array wash buffers. 1 ml of the conditioned medium is added into the well, and the antibody array membranes are incubated overnight at 4 °C. The array membranes are then washed twice with the wash buffers. 1 ml of the prepared Biotinylated Antibody Cocktail is pipetted into each well and incubated overnight at 4 °C. The membranes are washed twice with the wash buffers. 2 ml of the HRP-Streptavidin solution is added onto the membrane and incubated for 2 h at room temperature. After washing, the membranes are added with the chemiluminescent detection buffer mixture and transferred to an automated imaging system (UVP BioSpectrum 810, Thermo Fisher Scientific) to capture the images of the array spots. The antigen-specific antibody spots are analyzed and quantified using an image processing and analysis software, ImageJ (National Institutes of Health) with a MicroArray Profile plugin (https://www.optinav.info/MicroArray_Profile.htm).

2.10. Atomic force microscopy (AFM) analysis

Other than cytokines, physical properties also play important roles in regulating endothelial cell sprouting into the hydrogels. In the experiments, three 100 μl hydrogel samples without MRC-5 cells and three 100 μl hydrogels samples with MRC-5 cells (10⁶ cells/ml) are prepared in the wells punched by a 6 mm diameter biopsy punch on 1 mm thick PDMS

coating layers inside the conventional 3.5 cm petri-dishes (93,040, TPP Techno Plastic Products AG) and cultured using the HUVEC medium for 72 h. The biological atomic force microscopy (Bio-AFM) (JPK NanoWizard 3, Bruker Nano GmbH, Berlin, Germany) is then exploited to measure the elasticities of the hydrogels cultured without and with the MRC-5 cells covered by the medium. In the measurement, a four-side pyramid tip (PNP-TR20, Nanoworld, Neuchâtel, Switzerland) is used under the QI mode of the Bio-AFM setup (JPK NanoWizard Control, Bruker Nano GmbH) as an indenter to scan across a $30 \times 30 \mu\text{m}^2$ area of the samples. To ensure accurate measurement of the elasticity, the maximum indentation depth of 4000 nm and maximum indentation force of 5 nN are set for the measurement. During the scanning, the force-displacement curve measured at each indentation pixel is collected and further used to calculate the Young's modulus of each position of the hydrogel samples by optimum curve fitting according to the Hertz model [23].

2.11. Statistical analysis

A Student's t-test is performed to statistically analyze the difference between the control (uniform oxygen concentration) and experimental (with oxygen gradients) groups, data are analyzed from brightfield images and cell viability fluorescence images. If the *P* value is less than 0.05, the difference is considered significant (*: $p < 0.05$; **: $p < 0.01$; ***: $p < 0.001$). One-way ANOVA is applied to investigate the angiogenic sprouting area length differences under three types of wall widths. Numerical values are expressed as means \pm SDs of more than three independent experiments.

3. Results

3.1. Oxygen gradient profiles in the microfluidic devices

In order to investigate the actual oxygen tension profiles generated inside the hydrogel and cell culture channels, the oxygen sensitive fluorescence dye and the widefield frequency domain fluorescence lifetime image microscopy (FD-FLIM) measurement system are utilized for quantitative characterization [23]. Fig. 3(a) shows the fluorescence lifetime image experimentally measured using the FD-FLIM in the microfluidic device with a $50 \mu\text{m}$ -wide wall between the oxygen scavenging channel and the hydrogel channel. The image shows that the lifetime of the dye is longer in the area on the left side due to the lower oxygen tension resulted from the oxygen scavenging chemical reaction in the neighboring chemical reaction channel.

In addition, the oxygen tension profile can be further quantified according to the measured lifetime and the Stern-Volmer equation. The detailed calculation procedure has been previously described in the

published works [23,31]. The calculated result is plotted in Fig. 3(a). The plot shows the oxygen gradient can be successfully established along the width of the hydrogel and cell culture channels. For the device with $50 \mu\text{m}$ -wide wall between the oxygen scavenging channel and the hydrogel channel, the oxygen can be reduced to lower than 1% on the left side.

To compare the oxygen gradient profiles established in the devices with different wall widths (50 , 75 , and $100 \mu\text{m}$) between the oxygen scavenging channels and the hydrogel channels, Fig. 3(b) plots the oxygen tension profiles in the devices with three different dimensions. The generated oxygen gradients range from 0.6%–14.8%, 2.0%–15.4% and 3.9%–17.4% in the devices with the wall widths of 50 , 75 , and $100 \mu\text{m}$, respectively. The results indicate that the oxygen tensions can be lowered by decreasing the wall width between the oxygen scavenging channel and the hydrogel channel. In addition, to confirm the long-term stability of the generated oxygen gradients, the oxygen gradients established in the same device at different time points are also measured. Fig. S3(a) in the Supplementary Information shows the oxygen tension profiles calculated from the measured fluorescence lifetime using the FD-FLIM at 5 time points (0.5, 3, 8, 24, 72 h). The quantitative data as show in Fig. S3(b) plots the average oxygen tension along each *x* position. The results show that the oxygen tension values at the same *x* position at different time points are similar to each other, and the differences are no larger than 1% confirming the great long-term stability of the device for oxygen gradient generation.

3.2. Cell viability analysis

To confirm the cell culture compatibility of the device and observe the cell viability under various oxygen gradients, fluorescence-based cell viability assays are performed in the experiments. Fig. 4(a) and (b) show the brightfield phase and fluorescence images of the fluorescently stained HUVECs cultured within the devices (wall width of $50 \mu\text{m}$) for a period of 72 h under normoxia and the oxygen gradient, respectively. The images show that the HUVECs can attach well on the substrate during the 3-day culture for both conditions. Furthermore, the sprouting of the HUVECs into the hydrogel can be observed in the experiment with the oxygen gradient. In addition, the images show that the majority of the cells show green fluorescence from the Calcein AM labeling the live cells suggesting that the cell can maintain great viability after culture under different oxygen microenvironments (normoxia and the oxygen gradient) for 3 days.

To further quantify the cell viability assay results, image analysis is performed to enumerate live numbers and total cell numbers on the fluorescence images. Fig. 4(c) plots the quantification and statistically analyzed results showing the viabilities of the HUVECs cultured within the devices under different oxygen microenvironments. The results indicate that the cell viabilities for all the cell culture conditions are

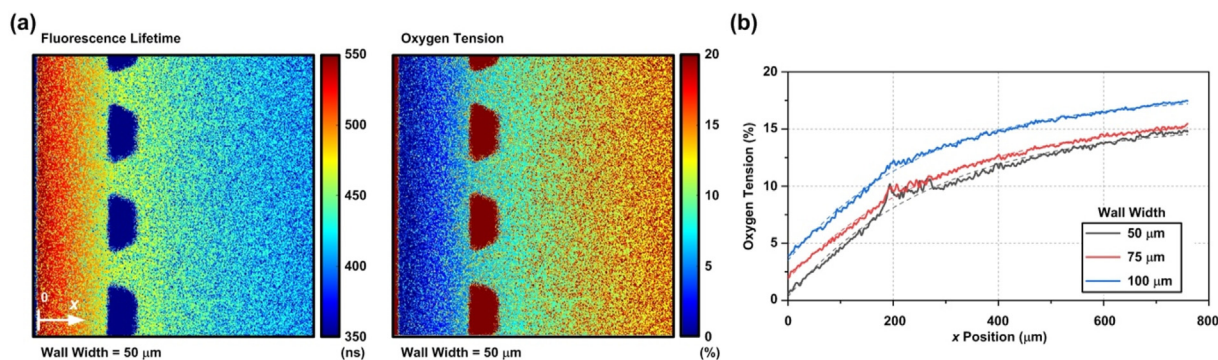


Fig. 3. (a) The measured fluorescence lifetime and the calculated oxygen gradient profile within a microfluidic device with a $50 \mu\text{m}$ -wide wall between the oxygen scavenging channel and the hydrogel channel in the experiment. (b) The measured average oxygen tension profiles within the microfluidic devices with three different wall widths.

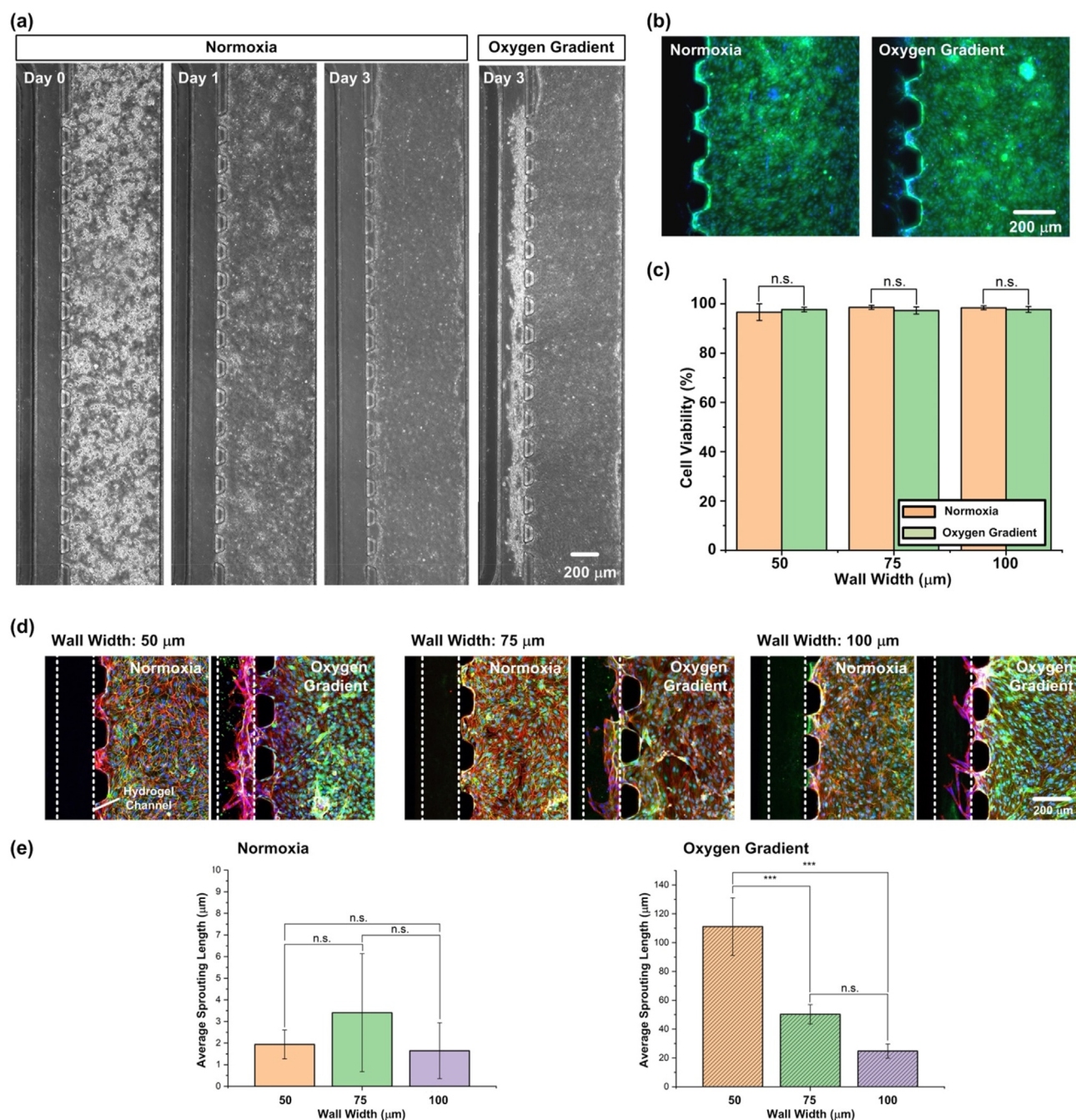


Fig. 4. (a) The brightfield phase images of the HUVECs cultured under normoxia on Day 0, 1, and 3; and the image of the HUVECs cultured under an oxygen gradient on Day 3. The width of the wall between the oxygen scavenging channel and the hydrogel channel is 50 μm. (b) The fluorescence images of the HUVECs stained with live/dead fluorescent dyes (green: Calcein AM for live cells; red: Ethd-1 for dead cells; blue: Hoechst 33,342 for nuclei) cultured under normoxia and the oxygen gradient on Day 3. (c) Quantified viabilities of the HUVECs on Day 3 cultured under normoxia and oxygen gradients generated in the devices. (d) Confocal images of the HUVECs cultured under various oxygen microenvironments generated using the devices with the different wall widths between the oxygen scavenging channels and the hydrogel channels (green: VE-cadherin; red: F-actin; blue: nuclei). (e) The estimated average lengths of the HUVECs sprouting into the hydrogels under normoxia and various oxygen gradients generated in the devices. The results significantly different from the normoxia (control) experiments are labeled with asterisk symbols (*: $p < 0.05$; **: $p < 0.01$; ***: $p < 0.001$). Data are expressed as the mean \pm standard deviation ($n = 3$).

higher than 95%, and no statistical differences between the cell viabilities obtained from the experiments under the normoxia and the oxygen gradient microenvironments in the devices with identical geometries. The results confirm the great cell compatibility of the microfluidic device and the functionality of the oxygen gradient generation scheme, and also suggest that the cells live well under various oxygen microenvironments established in the microfluidic devices.

3.3. Sprouting of HUVECs under different oxygen microenvironments

In the experiments, the effects of the oxygen gradients on endothelial cell sprouting into three-dimensional hydrogels are first studied. Fig. 4(d) shows the confocal images (maximum intensity projection) of the HUVECs cultured under normoxia and oxygen gradients in the microfluidic devices with three different wall widths between the oxygen scavenging channels and the hydrogel channels. The cells are stained

with adherens junction protein, VE-cadherin (green), cytoskeleton, f-actin (red), and nuclei (blue). The images show that the VE-cadherin expresses at the cell-to-cell junctions suggesting that HUVECs can form endothelium with great integrity in the cell culture channels under all the culture conditions. In all the experiments performed under normoxia, the HUVECs tend not to sprout into the hydrogel after the 3-day culture. In contrast, the HUVECs sprouting into the hydrogels is observed from the experiments performed with the oxygen gradients. Moreover, the length of the HUVECs sprouting into the hydrogel becomes greater for the device with the narrower wall widths leading to the similar oxygen gradient profiles but with lower oxygen tension values. Also, the cells sprouting into the hydrogel show abundant f-actin expression.

The areas of the HUVECs sprouting into the hydrogels are automatically quantified based on the brightfield images using the computer codes. The average sprouting lengths (L_{SA}) are then calculated based on the aforementioned equation, and the results are plotted in Fig. 4(e). The results indicate that the cell sprouting length possesses no significant differences among the devices with different wall widths under the normoxia culture condition, and all the average cell sprouting lengths are no greater than 3.5 μm . In comparison, the cell sprouting length can be affected by the oxygen gradient profiles established in the devices with different wall widths. The average sprouting lengths are 111.1, 50.3, and 24.7 μm for the devices with wall widths of 50, 75, and 100 μm , respectively. The results indicate that the sprouting lengths significantly increase when the HUVECs are cultured under the oxygen gradients with lower oxygen tensions established in the microfluidic devices with narrower wall widths. The sprouting lengths obtained from the experiments conducted under normoxia and the oxygen gradients are further compared. The results reveal that using the devices with the wall widths of 50, 75, and 100 μm , the sprouting lengths are 48.3, 21.8, and 10.7 times as the average values obtained from all the experiments performed

without the oxygen gradients in the devices with three different dimensions on Day 3, respectively. The statistically greater sprouting lengths suggest that the critical roles of the oxygen gradient in endothelial cell sprouting into the three-dimensional hydrogels.

3.4. Sprouting of HUVECs with co-culture of MRC-5 cells in the hydrogel

To further investigate the role of stromal cells in endothelial cell sprouting, co-culture of fibroblast cells is performed in the experiments. The human fetal lung fibroblast cells (MRC-5) are cultured in the hydrogels located in the hydrogel channel within the microfluidic device. For simplification, the co-culture experiments are all performed in the device with the 50 μm -wide wall between the hydrogel channel and the oxygen scavenging channel for comparison. The effects of the MRC-5 cells cultured in the hydrogel on the oxygen gradient profile are first investigated in the experiments. The oxygen tension profiles on the same device containing the MRC-5 cells in the hydrogel are characterized for 3 days. The measured results are compared to the gradients measured on the device without the cells, and the results are shown in Fig. S4 in the Supplementary Information. The results suggest that the MRC-5 cells cultured in the hydrogel have minimal effects on the oxygen gradients generated using the chemical reaction method, and the stable oxygen gradients can be maintained in the devices with or without the MRC-5 cells cultured in the hydrogel.

Fig. 5(a) shows the brightfield phase images of co-culture of the HUVECs and the MRC-5 cells within the devices under normoxia and the oxygen gradient conditions on Day 1 and 3. The images show that both cell types can live well in the devices, and the HUVECs sprout into the hydrogels under both oxygen microenvironments. Fig. 5(b) shows the confocal images (maximum intensity projection) of the cells cultured in the microfluidic devices on Day 3. For the experiments without co-

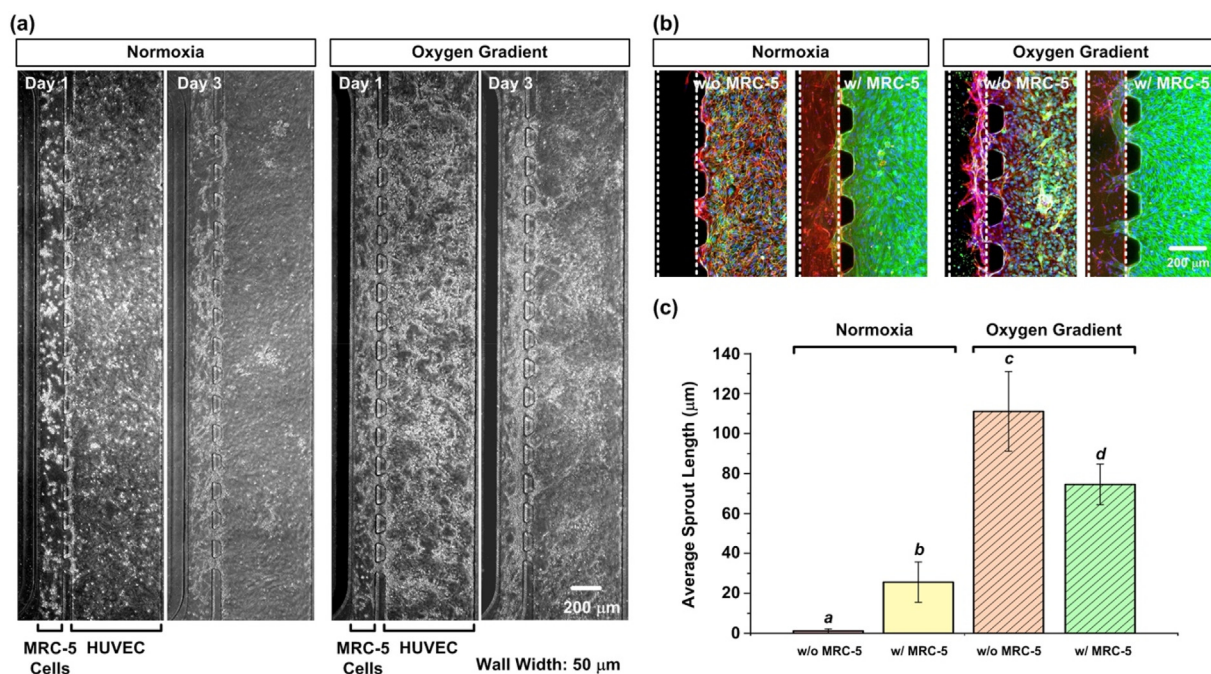


Fig. 5. (a) The brightfield phase images of the HUVECs co-cultured with the MRC-5 cells in the hydrogels under normoxia and the oxygen gradients on Day 1 and Day 3 in the microfluidic devices with 50 μm -wide walls between the oxygen scavenging channels and the hydrogel channels. (b) Confocal images of the HUVECs cultured without and with MRC-5 cells in the hydrogels under normoxia and the oxygen gradients on Day 3. In the experiments without co-culture of MRC-5 cells, the VE-cadherin (green), F-actin (red), and nuclei (blue) of the HUVECs are fluorescently stained. In order to differentiate different cell types in the co-culture experiments, the HUVECs and the MRC-5 cells are fluorescently labeled using CD31 (green) and CellTracker Red CMTPX (red), respectively. The nuclei of both cell types are also fluorescently labeled (blue). (c) The estimated average length of the HUVECs sprouting into the hydrogels under different culture conditions. Different letters represent a significant difference between the co-culture conditions and the oxygen microenvironments (a, b, c, d = $p < 0.05$). Data are expressed as the mean \pm standard deviation ($n = 3$).

culture of the MRC-5 cells, the HUVECs are stained with VE-cadherin (green), f-actin (red), and nuclei (blue). In the co-culture experiments, the HUVECs and the MRC-5 cells are labeled using CD31 (green) and CellTracker Red CMTPX (red) for cell type differentiation, respectively. Under the normoxia condition, the presence of MRC-5 can promote the HUVECs sprouting into the hydrogels making the average sprout lengths increase from 1.1 to 25.6 μm . When the oxygen microenvironment changes from normoxia to the oxygen gradient, the sprouting lengths can be further increased. The sprouting lengths increase from 1.1 and 25.6 μm to 111.1 and 74.5 μm for the HUVECs cultured without and with the MRC-5 cells, respectively. The results suggest that both oxygen gradient and co-culture of the stromal cells do promote the sprouting of HUVECs into the hydrogel; however, the two factors are not synergistic. Comparing the results performed in the device with the wall width of 50 μm , the sprouting length greatly increases more than a hundred times when the culture environment changes from normoxia to the oxygen gradient albeit the HUVECs are not cultured with the MRC-5 cells. In contrast, the length only increases about 2.9 times in the HUVEC/MRC-5 cell co-culture experiments. In addition, comparing the results obtained from the experiments with the oxygen gradients, the average sprouting length of the HUVECs co-cultured with the MRC-5 cells is 74.5 μm which is about 32.9% than that of the HUVECs cultured alone (about 111.1 μm). Furthermore, the images show that the morphologies of the HUVECs sprouting into the hydrogels are different in the experiments without and with co-culture of MRC-5 cells. In the co-culture experiments, the HUVECs tend to form tubular structures with larger diameters.

3.5. Cytokine array analysis

The cytokine array analysis is conducted to investigate the cytokine secretion difference among the cell experiments performed under different oxygen microenvironments (normoxia and oxygen gradient) and co-culture conditions (without and with MRC-5 cells). The images of

the cytokine arrays obtained from different experimental conditions are shown in Fig. 6(a), and the quantitative results of all the cytokines analyzed in the array are shown in Fig. S2(b) in the Supplementary Information. The images highlight the six angiogenesis-related cytokines having distinct expression levels among the experimental conditions, including: angiogenin, epithelial-neutrophil activating peptide 78 (ENA-78), interleukin 6 (IL-6), placenta growth factor (PIGF), transforming growth factor β 1 (TGF β -1), and vascular endothelial growth factor D (VEGF-D). Fig. 6(b) shows the quantified results calculating the integrated intensities normalized to the control experiment (culture of HUVEC under normoxia without MRC-5 cells). The plots show that concentrations of pro-angiogenesis cytokines: angiogenin, ENA-78, and IL-6 are greatly elevated for more than 34%, 104%, and 270% in the medium of the HUVECs cultured with MRC-5 cells in the hydrogels, respectively. Furthermore, the angiogenin and ENA-78 concentrations are further increased when the cells are co-cultured under the oxygen gradient comparing to normoxia. In contrast, the IL-6 cytokine with broad-ranging effects is slightly decreased when the co-culture is performed under the oxygen gradient. The results suggest that co-culture with the fibroblast cells promotes the secretion of the pro-angiogenesis cytokines angiogenin, ENA-78, and IL-6. Furthermore, culture under the oxygen gradient environment has synergistic effects to further increase the secretion of angiogenin and ENA-78.

In addition, when the HUVECs are co-cultured with the MRC-5 cells, the secretion of PIGF, a multitasking cytokine and a member of the VEGF family [33] is decreased by more than 50% under normoxia. No matter the HUVECs cultured without or with MRC-5 cells, the PIGF secretion is increased when the cells experience the oxygen gradients. Similarly, VEGF-D secretion is decreased by about 20% when the MRC-5 cells are present in the hydrogel under normoxia, and is increased when the cells are cultured under the oxygen gradient. TGF β -1 belongs to the TGF β superfamily having important regulatory roles in many cellular functions like proliferation, differentiation, apoptosis, chemotaxis, and

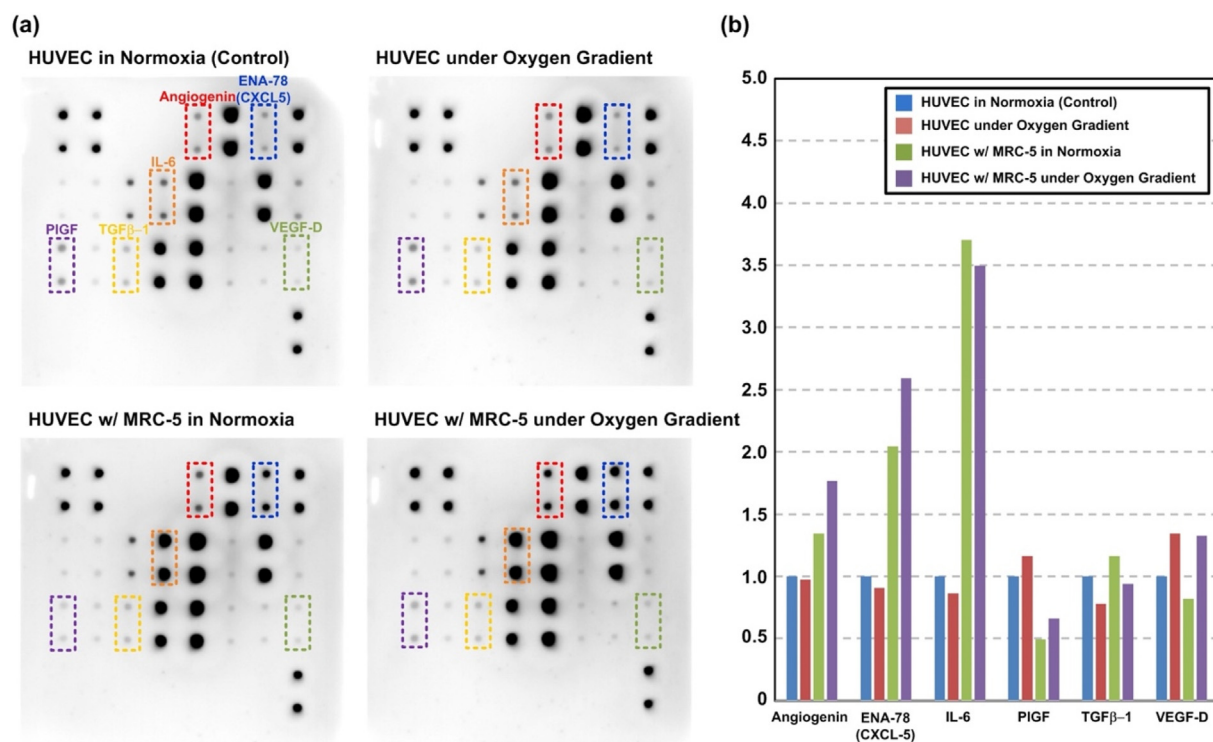


Fig. 6. (a) Images of the angiogenesis cytokine arrays showing different cytokine patterns among the experiments performed under different oxygen microenvironments (normoxia and oxygen gradient) and co-culture conditions (without and with MRC-5 cells). (b) Normalized integrated intensities of the cytokines vary under different oxygen microenvironments and cell co-culture conditions.

angiogenesis. In the experiment, TGF β -1 secretion slightly increases (approximately 16–20%) when the HUVECs are cultured with the MRC-5 cells. In contrast, the TGF β -1 secretion decreases when the cells are cultured under the oxygen gradients (approximately 20% comparing to the normoxia condition) regardless of the co-culture condition. The results suggest that co-culture with MRC-5 and the oxygen gradient have the opposite effect on the TGF β -1 secretion.

3.6. AFM analysis

Other than cytokines, the physical properties of hydrogels may also play important roles in regulating endothelial cell sprouting. To characterize the elasticity of the hydrogels without and with MRC-5 cells cultured in them, atomic force microscopy is performed to quantify the elasticity of the hydrogels. Fig. 7(a) shows the spatial distributions of the elasticity values measured using the AFM with $30\ \mu\text{m} \times 30\ \mu\text{m}$ areas on the hydrogels without and with MRC-5 cells. The images show that both hydrogels possess non-uniform elasticity distributions, and the one with MRC-5 cells has higher elasticity comparing to that without the MRC-5 cells. To further quantitatively compare the elasticities of both hydrogels,

the histograms and the average values of the elasticity values are further plotted in Fig. 7(b). The histograms show that most of the elasticity values of the hydrogel without the MRC-5 cells are smaller than 4 kPa. In contrast, the elasticity values of the hydrogel with the MRC-5 cells mainly distribute between 4 and 8 kPa. The average elasticity values of the hydrogels without and with the MRC-5 cells are approximately 2.2 and 5.9 kPa, respectively.

4. Discussion

The results confirm the functionality of the developed device for investigating the effects of oxygen gradients and stromal cell co-culture on the sprouting angiogenesis, and indicate the key roles of the two factors and their combination. The experimental observation suggests that either the oxygen gradient, co-culture of MRC-5 cells, or their combination can promote the sprouting angiogenesis. When the endothelial cells are cultured under the oxygen gradients, it has been found that the endothelial cells tend to collectively migrate toward to lower oxygen tension sites on a substrate under the oxygen gradients, and the proliferation can be promoted [23,24]. The similar oxygen

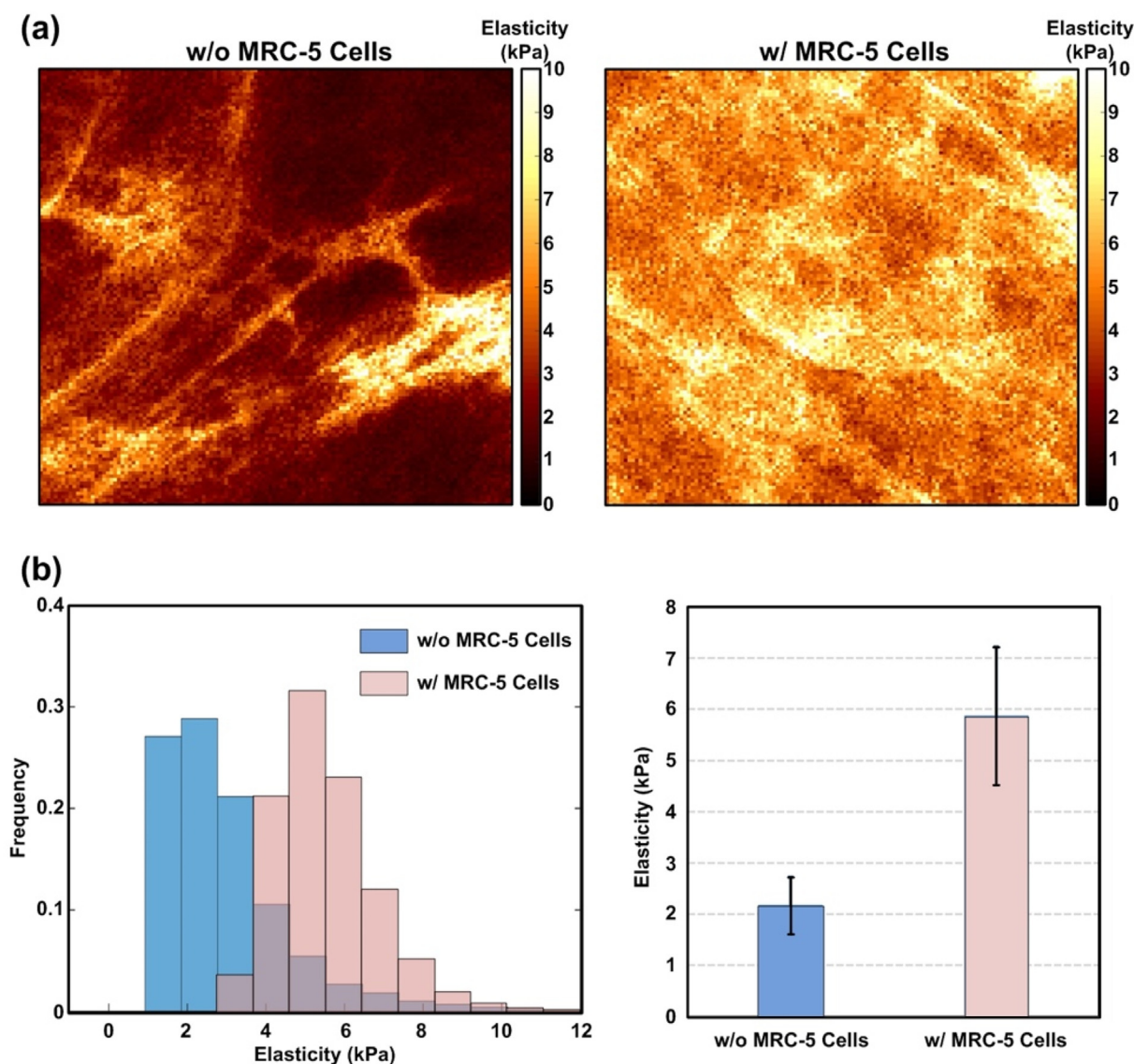


Fig. 7. (a) The spatial distribution of the elasticity values obtained from AFM measurements within $30\ \mu\text{m} \times 30\ \mu\text{m}$ areas (128×128 data points) on the hydrogel samples without and with MRC-5 cells cultured in them respectively. (b) Comparison of the histograms and the average values ($n = 10$) of the elasticities estimated from the AFM measurement on the hydrogel samples without and with the MRC-5 cells.

gradient-driven cellular response has also been found on the HUVECs sprouting into the three-dimensional hydrogel matrix in the experiments. Furthermore, under similar oxygen gradient slopes, the HUVECs sprout into the matrix with higher rates under the lower oxygen tension values.

The cytokine assay results show that expression of PlGF and VEGF-D proteins belonging to the proangiogenic VEGF family increase during the HUVEC culture under the oxygen gradients without or with MRC-5 co-culture [34]. PlGF has been found to be highly expressed in endothelial cells and identified as a multitasking cytokine that can affect the activities of various cells including endothelial cells and fibroblasts [33,35]. On the endothelial cells, VEGF receptor-1 (VEGFR-1) has been identified as the receptor for PlGF [36]. PlGF can induce endothelial cell migration and proliferation, and also promote vascular remodeling toward a normal phenotype [37,38]. Furthermore, PlGF is found to support the proliferation of fibroblasts promoting vessel maturation [39]. In addition, previous data have shown that hypoxia increases endothelial cell PlGF expression post-transcriptionally [35], and similar positive modulation of PlGF expression under hypoxia has also been observed in other cell types including fibroblasts [38,40]. VEGF-D is also a member of the VEGF family, and it can promote the remodeling of blood vessels in the development and disease [33]. Different from PlGF, the receptors of VEGF-D are VEGFR-2 and VEGFR-3, which can regulate angiogenesis and lymphangiogenesis, respectively [41]. Both VEGFR-1 and VEGFR-2 are required for normal development and angiogenesis [42]. It has been identified that VEGF-D plays a key role in new blood vessel growth, and stimulates proliferation and migration of endothelial cells *in vitro* as other members of the VEGF family. Recent studies also reveal that the expression of VEGF-D is tightly linked to hypoxia, which activates its expression at both transcriptional and translational levels [43].

In contrast, the expression of TGF β is downregulated when the HUVECs are cultured under the oxygen gradients. It has been found that TGF β family is a crucial regulatory factor in many cellular functions and biological processes, such as proliferation, differentiation, migration, apoptosis, wound healing, and angiogenesis [44,45]. TGF β is considered as a key factor during vascular remodeling and the disintegration phase of angiogenesis, which is generally recognized as an inhibitor of angiogenesis [46]. Furthermore, TGF- β can decrease cell growth and further lead to cell cycle arrest in most normal cells and early-stage of cancers [47]. The mechanisms of TGF β family proteins as the role of being anti- or pro-angiogenic factors during blood vessel formation processes are still unclear. TGF β -1 has been found to induce angiogenesis *in vivo* [48–50]; however, it has also been shown that TGF β inhibits certain endothelial cellular functions including cell proliferation, migration and proteolytic activity *in vitro* [51–53]. When endothelial cells are exposed to hypoxia, it is demonstrated that messenger RNA and protein levels of TGF β -2, a cytokine with potent regulatory effects on vascular inflammatory responses, are increased [54]. The increased TGF β level contradicts to the observation from the oxygen gradient experiments in this research. The effects of oxygen gradient besides lowered oxygen tension values on the cytokine expression variation during sprouting angiogenesis are still not clear. Further investigation is desired to decipher the underlying mechanisms of the observed oxygen gradient mediated cellular response.

The role of fibroblasts in angiogenesis has been recognized under physiological and pathological conditions [12]. In the experiments, when the HUVECs are co-cultured with the MRC-5 fibroblasts, it is observed that the expression of angiogenin, ENA-78 (i.e., C-X-C motif chemokine ligand 5, CXCL5), and IL-6 are increased, while the PlGF level is decreased. Angiogenin and ENA-78 have been identified as potential angiogenic promoting cytokines. Angiogenin is found to support endothelial and fibroblast cell adhesion [55], and it can also induce angiogenesis by activating endothelial cells and triggering cell migration, invasion, proliferation, and formation of tubular structures [56]. ENA-78 can be secreted by fibroblasts, and it has been found to promote angiogenesis through various pathways [57,58]. For IL-6, its potential as an angiogenic agent has not been fully investigated. In a recent study, it has

been found that IL-6 can directly induce blood vessel sprouting, endothelial cell proliferation and migration as VEGF. However, IL6-stimulated vessel sprouts can be defective compared with VEGF-stimulated ones [59]. In contrast, PlGF concentration is decreased when the HUVECs are co-cultured with the MRC-5 cells. Since the PlGF is most highly expressed in endothelial cells [35], the concentration decrease may be resulted from the uptake by the fibroblast cells.

The co-culture of fibroblast in the experiments not only provides additional cytokines but also alters the hydrogel elasticity. The physical property of the hydrogel extracellular matrix (ECM) has been identified as a pivotal factor in affecting the sprouting angiogenesis and lumen formation of the endothelial cells [12]. Stiffness of the hydrogel has been shown to affect the cell proliferation, signaling and differentiation on endothelial cells [60–62] and to regulate cell formation during angiogenic processes [63]. Furthermore, it is noticed that sprouting angiogenesis and sprouting distance can be promoted by increasing the stiffness of the ECM [63]. The microelasticities of normal healthy tissues from various organs have been characterized, and they range from one-tenth to several tens kPa [64]. In the experiments, the elasticity of the hydrogel without fibroblasts is estimated to be 2.2 kPa that is within the range of the normal tissues. It is found that sprouting angiogenesis is limited without oxygen gradient application or fibroblast co-culture, which agrees well with the reported observation. Since the co-culture of fibroblasts increases the elasticity of the hydrogel to 5.9 kPa, the sprouting angiogenesis can be greatly promoted. It is observed that the average sprouting distance increases more than 23 times resulted from increased hydrogel elasticity and additional cytokines secreted from the fibroblasts.

With the combination of the oxygen gradient culture environment and the co-culture of the MRC-5 fibroblasts, they have synergistic effects on increasing expression of pro-angiogenic factors angiogenin and ENA-78 and opposite effects on expression of IL-6, PlGF, and TGF β -1. Both oxygen gradient and co-culture of fibroblast promote sprouting angiogenesis. It is found that the sprouting distance is greater when the HUVECs are cultured under the oxygen gradients comparing to the co-culture experiments. However, the vascular lumen formation of the HUVECs cultured under the oxygen gradient is much less observed due to lower hydrogel elasticity and shortage of cytokines secreted from the fibroblasts such as angiogenin and ENA-78. The result confirms the critical role of fibroblasts in sprouting angiogenesis with better vessel formation from biomolecular and physical property viewpoints. The angiogenesis can be further promoted when the HUVECs are co-cultured with the fibroblasts under the oxygen gradient. The sprouting distance is further increased by approximately 2.9 times as that observed in the co-culture experiments without the oxygen gradient, and the HUVECs can still form vessel-like tubular structures as those observed in the co-culture experiments. Additionally, the decrease of IL-6 and TGF β -1 when the HUVECs co-cultured with fibroblasts under oxygen gradients may help the endothelial cells to form less defective blood vessels in a more physiological-like condition. The developed device can greatly help to advance the sprouting angiogenesis research under the effects of *in vivo*-like oxygen gradients, and more exploration can be conducted to better study the sprouting angiogenesis under various physiological and pathological conditions.

5. Conclusion

In this paper, a microfluidic device capable of integrating a hydrogel matrix for cell culture and generating stable oxygen gradients is developed to study the sprouting angiogenesis of endothelial cells. The endothelial cells can be cultured as a monolayer endothelium inside the device to mimic an existing blood vessel, and the hydrogel without or with fibroblast cells cultured in it provides a matrix next to the formed endothelium for three-dimensional sprouting of the endothelial cells. Taking advantage of the spatially-confined chemical reaction method, the oxygen gradient can be established inside the device for cell culture.

Consequently, the sprouting angiogenesis under combinations of oxygen gradients and co-culture of fibroblast cells can be systematically studied using the device. In the experiments, the established oxygen gradients are quantitatively characterized, and the endothelial cell sprouting areas are estimated by imaging analysis. In addition, the cytokine array is performed to observe the cytokine variation among different experimental conditions, and the AFM is exploited to investigate the mechanical property change of the hydrogel matrix due to its remodeling. The results confirm the functionality provided by the device, and the critical roles of the oxygen gradients and co-culture of fibroblast cells to affect the cytokine compositions in the cell microenvironments and promote sprouting angiogenesis into the three-dimensional matrix. Using the developed device, sprouting angiogenesis can be systematically investigated to better explore blood vessel formation under various physiological and pathological conditions.

Credit author statement

Heng-Hua Hsu: Methodology, Investigation, Formal Analysis, Writing – Original Draft. Ping-Kiang Ko: Investigation, Formal Analysis, Visualization. Chien-Chung Peng: Investigation, Formal Analysis. Ya-Jen Cheng: Investigation. Hsiao-Mei Wu: Investigation, Formal Analysis, Writing – Review & Editing. Yi-Chung Tung: Conceptualization, Writing – Review & Editing, Visualization, Supervision, Project Administration, Funding Acquisition.

Declaration of competing interest

The authors declare that they have no known competing financial interests or personal relationships that could have appeared to influence the work reported in this paper.

Data availability

Data will be made available on request.

Acknowledgments

This paper is based on the work supported by the Taiwan National Science and Technology Council (NSTC 110-2221-E-001-005-MY3 and 111-2221-E-001-004-MY2), the Academia Sinica Career Development Award (AS-CDA-106-M07), and the Academia Sinica Neuroscience Core Facility (AS-CFII-110-101).

Appendix A. Supplementary data

Supplementary data to this article can be found online at <https://doi.org/10.1016/j.mtbio.2023.100703>.

References

- [1] T.H. Adair, J.P. Montani, *Angiogenesis*, 2010. San Rafael (CA).
- [2] B.W. Wong, E. Marsch, L. Treps, M. Baes, P. Carmeliet, Endothelial cell metabolism in health and disease: impact of hypoxia, *EMBO J.* 36 (15) (2017) 2187–2203.
- [3] J. Pauty, R. Usuba, I.G. Cheng, L. Hespel, H. Takahashi, K. Kato, M. Kobayashi, H. Nakajima, E. Lee, F. Yger, F. Soncin, Y.T. Matsunaga, A vascular endothelial growth factor-dependent sprouting angiogenesis assay based on an in vitro human blood vessel model for the study of anti-angiogenic drugs, *EBioMedicine* 27 (2018) 225–236.
- [4] J.E. Bader, K. Voss, J.C. Rathmell, Targeting metabolism to improve the tumor microenvironment for cancer immunotherapy, *Mol. Cell.* 78 (6) (2020) 1019–1033.
- [5] K. De Bock, M. Georgiadou, S. Schoors, A. Kuchnio, B.W. Wong, A.R. Cantelmo, A. Quaegebeur, B. Ghesquiere, S. Cauwenberghs, G. Eelen, L.K. Phng, I. Betz, B. Tembuyser, K. Brepoels, J. Welti, I. Geudens, I. Segura, B. Cruys, F. Bifari, I. Decimo, R. Blanco, S. Wyns, J. Vangindertael, S. Rocha, R.T. Collins, S. Munck, D. Daelemans, H. Imamura, R. Devlieger, M. Rider, P.P. Van Veldhoven, F. Schuit, R. Bartrons, J. Hofkens, P. Fraisl, S. Telang, R.J. Deberardinis, L. Schoonjans, S. Vinckier, J. Chesney, H. Gerhardt, M. Dewerchin, P. Carmeliet, Role of PKFB3-driven glycolysis in vessel sprouting, *Cell* 154 (3) (2013) 651–663.
- [6] F. Bordeleau, B.N. Mason, E.M. Lollis, M. Mazzola, M.R. Zanotelli, S. Somasegar, J.P. Califano, C. Montague, D.J. LaValley, J. Huynh, N. Mencia-Trinchant, Y.L. Negron Abril, D.C. Hassane, L.J. Bonassar, J.T. Butcher, R.S. Weiss, C.A. Reinhart-King, Matrix stiffening promotes a tumor vasculature phenotype, *Proc. Natl. Acad. Sci. U. S. A.* 114 (3) (2017) 492–497.
- [7] P. Fraisl, M. Mazzone, T. Schmidt, P. Carmeliet, Regulation of angiogenesis by oxygen and metabolism, *Dev. Cell* 16 (2) (2009) 167–179.
- [8] A. Costa, A. Scholer-Dahirel, F. Mechta-Grigoriou, The role of reactive oxygen species and metabolism on cancer cells and their microenvironment, *Semin. Cancer Biol.* 25 (2014) 23–32.
- [9] G. Eelen, L. Treps, X. Li, P. Carmeliet, Basic and therapeutic aspects of angiogenesis updated, *Circ. Res.* 127 (2) (2020) 310–329.
- [10] T. Hashimoto, F. Shibasaki, Hypoxia-inducible factor as an angiogenic master switch, *Front Pediatr* 3 (2015) 33.
- [11] B.L. Krock, N. Skuli, M.C. Simon, Hypoxia-induced angiogenesis: good and evil, *Genes Cancer* 2 (12) (2011) 1117–1133.
- [12] A.C. Newman, M.N. Nakatsu, W. Chou, P.D. Gershon, C.C. Hughes, The requirement for fibroblasts in angiogenesis: fibroblast-derived matrix proteins are essential for endothelial cell lumen formation, *Mol. Biol. Cell* 22 (20) (2011) 3791–3800.
- [13] I. Mahmud, D. Liao, DAXX in cancer: phenomena, processes, mechanisms and regulation, *Nucleic Acids Res.* 47 (15) (2019) 7734–7752.
- [14] S. Germain, C. Monnot, L. Muller, A. Eichmann, Hypoxia-driven angiogenesis: role of tip cells and extracellular matrix scaffolding, *Curr. Opin. Hematol.* 17 (3) (2010) 245–251.
- [15] R. Edmondson, J.J. Broglie, A.F. Adcock, L. Yang, Three-dimensional cell culture systems and their applications in drug discovery and cell-based biosensors, *Assay Drug Dev. Technol.* 12 (4) (2014) 207–218.
- [16] M. Mehling, S. Tay, Microfluidic cell culture, *Curr. Opin. Biotechnol.* 25 (2014) 95–102.
- [17] I. Meyvantsson, D.J. Beebe, Cell culture models in microfluidic systems, *Annu. Rev. Anal. Chem.* 1 (2008) 423–449.
- [18] Y. Kamotani, T. Bersano-Begey, N. Kato, Y.C. Tung, D. Huh, J.W. Song, S. Takayama, Individually programmable cell stretching microwell arrays actuated by a Braille display, *Biomaterials* 29 (17) (2008) 2646–2655.
- [19] M.C. Liu, H.C. Shih, J.G. Wu, T.W. Weng, C.Y. Wu, J.C. Lu, Y.C. Tung, Electrofluidic pressure sensor embedded microfluidic device: a study of endothelial cells under hydrostatic pressure and shear stress combinations, *Lab Chip* 13 (9) (2013) 1743–1753.
- [20] M.D. Brennan, M.L. Rexius-Hall, L.J. Elgass, D.T. Eddington, Oxygen control with microfluidics, *Lab Chip* 14 (22) (2014) 4305–4318.
- [21] C.W. Chang, Y.J. Cheng, M. Tu, Y.H. Chen, C.C. Peng, W.H. Liao, Y.C. Tung, A polydimethylsiloxane-polycarbonate hybrid microfluidic device capable of generating perpendicular chemical and oxygen gradients for cell culture studies, *Lab Chip* 14 (19) (2014) 3762–3772.
- [22] Y.A. Chen, A.D. King, H.C. Shih, C.C. Peng, C.Y. Wu, W.H. Liao, Y.C. Tung, Generation of oxygen gradients in microfluidic devices for cell culture using spatially confined chemical reactions, *Lab Chip* 11 (21) (2011) 3626–3633.
- [23] H.H. Hsu, P.L. Ko, H.M. Wu, H.C. Lin, C.K. Wang, Y.C. Tung, Study 3D endothelial cell network formation under various oxygen microenvironment and hydrogel composition combinations using upside-down microfluidic devices, *Small* 17 (15) (2021), e2006091.
- [24] H.C. Shih, T.A. Lee, H.M. Wu, P.L. Ko, W.H. Liao, Y.C. Tung, Microfluidic collective cell migration assay for study of endothelial cell proliferation and migration under combinations of oxygen gradients, tensions, and drug treatments, *Sci. Rep.* 9 (1) (2019) 8234.
- [25] H. Lee, W. Park, H. Ryu, N.L. Jeon, A microfluidic platform for quantitative analysis of cancer angiogenesis and intravasation, *Biomicrofluidics* 8 (5) (2014), 054102.
- [26] S. Kim, H. Lee, M. Chung, N.L. Jeon, Engineering of functional, perfusable 3D microvascular networks on a chip, *Lab Chip* 13 (8) (2013) 1489–1500.
- [27] Y.H. Chen, C.C. Peng, Y.C. Tung, Flip channel: a microfluidic device for uniform-sized embryoid body formation and differentiation, *Biomicrofluidics* 9 (5) (2015), 054111.
- [28] J.W. Song, L.L. Munn, Fluid forces control endothelial sprouting, *Proc. Natl. Acad. Sci. U. S. A.* 108 (37) (2011) 15342–15347.
- [29] J.H. Yeon, H.R. Ryu, M. Chung, Q.P. Hu, N.L. Jeon, In vitro formation and characterization of a perfusable three-dimensional tubular capillary network in microfluidic devices, *Lab Chip* 12 (16) (2012) 2815–2822.
- [30] G. Lazzari, V. Nicolas, M. Matsusaki, M. Akashi, P. Couvreur, S. Mura, Multicellular spheroid based on a triple co-culture: a novel 3D model to mimic pancreatic tumor complexity, *Acta Biomater.* 78 (2018) 296–307.
- [31] H.M. Wu, T.A. Lee, P.L. Ko, W.H. Liao, T.H. Hsieh, Y.C. Tung, Widefield frequency domain fluorescence lifetime imaging microscopy (FD-FLIM) for accurate measurement of oxygen gradients within microfluidic devices, *Analyst* 144 (11) (2019) 3494–3504.
- [32] W. Zhong, P. Urayama, M.A. Mycek, Imaging fluorescence lifetime modulation of a ruthenium-based dye in living cells: the potential for oxygen sensing, *J. Phys. D Appl. Phys.* 36 (14) (2003) 1689–1695.
- [33] M. Dewerchin, P. Carmeliet, PlGF: a multitasking cytokine with disease-restricted activity, *Cold Spring Harb Perspect Med* 2 (8) (2012).
- [34] M. Migdal, B. Huppertz, S. Tessler, A. Comforti, M. Shibuya, R. Reich, H. Baumann, G. Neufeld, Neupilin-1 is a placenta growth factor-2 receptor, *J. Biol. Chem.* 273 (35) (1998) 22272–22278.
- [35] L. Xiang, R. Varshney, N.A. Rashdan, J.H. Shaw, P.G. Lloyd, Placenta growth factor and vascular endothelial growth factor have differential, cell-type specific patterns of expression in vascular cells, *Microcirculation* 21 (5) (2014) 368–379.

- [36] D. Ribatti, The discovery of the placental growth factor and its role in angiogenesis: a historical review, *Angiogenesis* 11 (3) (2008) 215–221.
- [37] H. Iwamoto, Y. Zhang, T. Seki, Y. Yang, M. Nakamura, J. Wang, X. Yang, T. Torimura, Y. Cao, PlGF-induced VEGFR1-dependent vascular remodeling determines opposing antitumor effects and drug resistance to Dll4-Notch inhibitors, *Sci. Adv.* 1 (3) (2015), e1400244.
- [38] C.J. Green, P. Lichtlen, N.T. Huynh, M. Yanovsky, K.R. Laderoute, W. Schaffner, B.J. Murphy, Placenta growth factor gene expression is induced by hypoxia in fibroblasts: a central role for metal transcription factor-1, *Cancer Res.* 61 (6) (2001) 2696–2703.
- [39] S. De Falco, The discovery of placenta growth factor and its biological activity, *Exp. Mol. Med.* 44 (1) (2012) 1–9.
- [40] L. Tudisco, A. Orlandi, V. Tarallo, S. De Falco, Hypoxia activates placental growth factor expression in lymphatic endothelial cells, *Oncotarget* 8 (20) (2017) 32873–32883.
- [41] M. Shibuya, Vascular endothelial growth factor (VEGF) and its receptor (vegfr) signaling in angiogenesis: a crucial target for anti- and pro-angiogenic therapies, *Genes Cancer* 2 (12) (2011) 1097–1105.
- [42] N. Rahimi, VEGFR-1 and VEGFR-2: two non-identical twins with a unique physiognomy, *Front. Biosci.* 11 (2006) 818–829.
- [43] F. Morfoisse, E. Renaud, F. Hantelys, A.C. Prats, B. Garmy-Susini, Role of hypoxia and vascular endothelial growth factors in lymphangiogenesis, *Mol Cell Oncol* 1 (1) (2014), e29907.
- [44] D. Gazit, Y. Zilberman, G. Turgeman, S. Zhou, A. Kahn, Recombinant TGF-beta 1 stimulates bone marrow osteoprogenitor cell activity and bone matrix synthesis in osteopenic, old male mice, *J. Cell. Biochem.* 73 (3) (1999) 379–389.
- [45] J. Ma, G. Sanchez-Duffhues, M.J. Goumans, P. Ten Dijke, TGF-beta-Induced endothelial to mesenchymal transition in disease and tissue engineering, *Front. Cell Dev. Biol.* 8 (2020) 260.
- [46] M.S. Pepper, Transforming growth factor-beta: vasculogenesis, angiogenesis, and vessel wall integrity, *Cytokine Growth Factor Rev.* 8 (1) (1997) 21–43.
- [47] J. Massague, TGFbeta signalling in context, *Nat. Rev. Mol. Cell Biol.* 13 (10) (2012) 616–630.
- [48] A.B. Roberts, M.B. Sporn, R.K. Assoian, J.M. Smith, N.S. Roche, L.M. Wakefield, U.I. Heine, L.A. Liotta, V. Falanga, J.H. Kehrl, et al., Transforming growth factor type beta: rapid induction of fibrosis and angiogenesis in vivo and stimulation of collagen formation in vitro, *Proc. Natl. Acad. Sci. U. S. A.* 83 (12) (1986) 4167–4171.
- [49] J.A. Madri, B.M. Pratt, A.M. Tucker, Phenotypic modulation of endothelial cells by transforming growth factor-beta depends upon the composition and organization of the extracellular matrix, *J. Cell Biol.* 106 (4) (1988) 1375–1384.
- [50] E.Y. Yang, H.L. Moses, Transforming growth factor beta 1-induced changes in cell migration, proliferation, and angiogenesis in the chicken chorioallantoic membrane, *J. Cell Biol.* 111 (2) (1990) 731–741.
- [51] M.J. Pollman, L. Naumovski, G.H. Gibbons, Vascular cell apoptosis: cell type-specific modulation by transforming growth factor-beta1 in endothelial cells versus smooth muscle cells, *Circulation* 99 (15) (1999) 2019–2026.
- [52] O. Saksela, D. Moscatelli, D.B. Rifkin, The opposing effects of basic fibroblast growth factor and transforming growth factor beta on the regulation of plasminogen activator activity in capillary endothelial cells, *J. Cell Biol.* 105 (2) (1987) 957–963.
- [53] M.S. Pepper, D. Belin, R. Montesano, L. Orci, J.D. Vassalli, Transforming growth factor-beta 1 modulates basic fibroblast growth factor-induced proteolytic and angiogenic properties of endothelial cells in vitro, *J. Cell Biol.* 111 (2) (1990) 743–755.
- [54] H.O. Akman, H. Zhang, M.A. Siddiqui, W. Solomon, E.L. Smith, O.A. Batuman, Response to hypoxia involves transforming growth factor-beta2 and Smad proteins in human endothelial cells, *Blood* 98 (12) (2001) 3324–3331.
- [55] F. Sconcin, Angiogenin supports endothelial and fibroblast cell adhesion, *Proc. Natl. Acad. Sci. U. S. A.* 89 (6) (1992) 2232–2236.
- [56] X. Gao, Z. Xu, Mechanisms of action of angiogenin, *Acta Biochim. Biophys. Sin.* 40 (7) (2008) 619–624.
- [57] C. Chen, Z.Q. Xu, Y.P. Zong, B.C. Ou, X.H. Shen, H. Feng, M.H. Zheng, J.K. Zhao, A.G. Lu, CXCL5 induces tumor angiogenesis via enhancing the expression of FOXD1 mediated by the AKT/NF-kappaB pathway in colorectal cancer, *Cell Death Dis.* 10 (3) (2019) 178.
- [58] W. Zhang, H. Wang, M. Sun, X. Deng, X. Wu, Y. Ma, M. Li, S.M. Shuo, Q. You, L. Miao, CXCL5/CXCR2 axis in tumor microenvironment as potential diagnostic biomarker and therapeutic target, *Cancer Commun.* 40 (2–3) (2020) 69–80.
- [59] G. Gopinathan, C. Milagre, O.M. Pearce, L.E. Reynolds, K. Hodivala-Dilke, D.A. Leinster, H. Zhong, R.E. Hollingsworth, R. Thompson, J.R. Whiteford, F. Balkwill, Interleukin-6 stimulates defective angiogenesis, *Cancer Res.* 75 (15) (2015) 3098–3107.
- [60] C.O. Crosby, J. Zoldan, Mimicking the physical cues of the ECM in angiogenic biomaterials, *Regen Biomater* 6 (2) (2019) 61–73.
- [61] D.J. LaValley, M.R. Zanutelli, F. Bordeleau, W. Wang, S.C. Schwager, C.A. Reinhart-King, Matrix stiffness enhances VEGFR-2 internalization, signaling, and proliferation in endothelial cells, *Converg Sci Phys Oncol* 3 (2017).
- [62] T. Bertucci, S. Kakarla, D. Kim, G. Dai, Differentiating human pluripotent stem cells to vascular endothelial cells for regenerative medicine, tissue engineering, and disease modeling, *Methods Mol. Biol.* 2375 (2022) 1–12.
- [63] Y. Guo, F. Mei, Y. Huang, S. Ma, Y. Wei, X. Zhang, M. Xu, Y. He, B.C. Heng, L. Chen, X. Deng, Matrix stiffness modulates tip cell formation through the p-PXN-Rac1-YAP signaling axis, *Bioact. Mater.* 7 (2022) 364–376.
- [64] C.R. Pfeifer, C.M. Alvey, J. Irianto, D.E. Discher, Genome variation across cancers scales with tissue stiffness - an invasion-mutation mechanism and implications for immune cell infiltration, *Curr. Opin. Struct. Biol.* 2 (2017) 103–114.